npg

ORIGINAL PAPER

Profiling the molecular difference between *Patched*- and *p53*-dependent rhabdomyosarcoma

Roland Kappler[1], Regine Bauer[1], Julia Calzada-Wack[2], Michael Rosemann[2], Bernhard Hemmerlein[3] and Heidi Hahn*[1]

[1]*Institute of Human Genetics, University of Göttingen, Heinrich-Düker-Weg 12, Göttingen, Germany; [2]Institute of Pathology, GSF-National Research Center for Environment and Health, Neuherberg, Germany; [3]Department of Pathology, University of Göttingen, Göttingen, Germany*

Rhabdomyosarcoma (RMS) is a highly malignant tumor that is histologically related to skeletal muscle, yet genetic and molecular lesions underlying its genesis and progression remain largely unknown. In this study we have compared the molecular profiles of two different mouse models of RMS, each associated with a defined primary genetic defect known to play a role in rhabdomyosarcomagenesis in man. We report that RMS of heterozygous *Patched1 (Ptch1)* mice show less aggressive growth and a greater degree of differentiation than RMS of heterozygous *p53* mice. By means of cDNA microarray analysis we demonstrate that RMS in *Ptch1* mutants predominantly express a number of myogenic markers, including *myogenic differentiation 1*, *myosin heavy chain*, *actin*, *troponin* and *tropomyosin*, as well as genes associated with Hedgehog/Patched signaling like *insulin-like growth factor 2*, forkhead box gene *Foxf1* and the growth arrest and DNA-damage-inducible gene *Gadd45a*. In sharp contrast, RMS in *p53* mutants display higher expression levels of cell cycle-associated genes like *cyclin B1*, *cyclin-dependent kinase 4* and the proliferation marker Ki-67. These results demonstrate that different causative mutations lead to distinct gene expression profiles in RMS, which appear to reflect their different biological characteristics. Our results provide a first step towards a molecular classification of different forms of RMS. If the described differences can be confirmed in human RMS our results will contribute to a new molecular taxonomy of this cancer, which will be critical for gene mutation- and expression-specific therapy.
Oncogene advance online publication, 11 October 2004; doi:10.1038/sj.onc.1208133

Introduction

Rhabdomyosarcoma (RMS), the most common soft-tissue sarcoma in children, falls into the broader category of small blue round cell tumors (Wexler and Helman, 1997). The currently accepted histological classification scheme differentiates between embryonal (ERMS), botryoid, alveolar (ARMS) and pleomorphic RMS (Horn and Enterline, 1958). However, RMS exhibit a degree of heterogeneity in their clinical behavior and clinical outcome that cannot be explained by their histology alone (Dagher and Helman, 1999). The inability to predict the outcome of the disease requires an aggressive treatment regimen that comprises surgery, radiation therapy and chemotherapy (Dagher and Helman, 1999). The development of a less toxic therapy protocol that decreases long-term morbidity and reduces the risk for secondary neoplasms is therefore of the uttermost importance.

The development of new therapies of RMS has been hampered by a lack of knowledge about the basic molecular mechanisms involved in tumor formation. The difficulty in determining these molecular alterations is in part a result of the low incidence of RMS. Some molecular lesions, such as the chromosomal translocations in ARMS generating PAX3- and PAX7-FKHR fusion proteins (Shapiro *et al.*, 1993; Davis *et al.*, 1994), or the loss of imprinting (LOI) of *insulin-like growth factor 2* (*IGF2*) in ERMS (Scrable *et al.*, 1987; Zhan *et al.*, 1994) have already been described. However, neither transgenic mice overexpressing *Igf2* nor mice expressing *Pax3-FKHR* develop RMS (Sun *et al.*, 1997; Lagutina *et al.*, 2002), indicating that these genetic defects may not be the primary events in RMS formation. It is possible that additional genetic changes that do not occur in mice are required, or that the transgenes did not effectively target the appropriate tissue.

In this report we use mouse models to establish the specific molecular signatures of two different forms of RMS, each caused by a defined gene defect, that is, mutation in *p53* or *PTCH1*. Germline mutations in either the transcription factor *p53* or the sonic hedgehog receptor *PTCH1* lead to cancer syndromes, respectively, Li-Fraumeni (LFS) or Nevoid Basal Cell Carcinoma Syndrome (NBCCS), associated with increased incidence of RMS (Gorlin, 1987; Malkin *et al.*, 1990). In addition, mutation of *p53* and deregulation of the
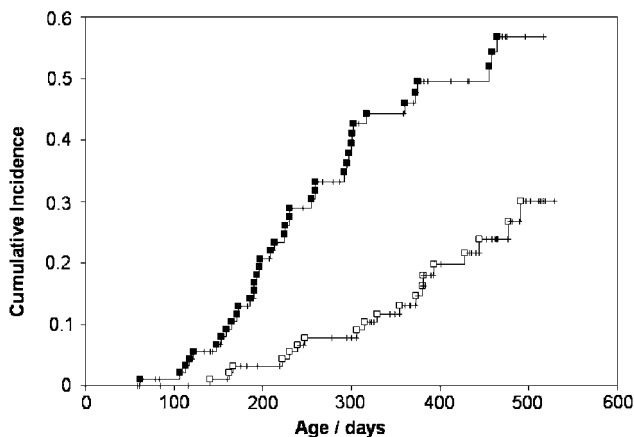
Hedgehog/Patched signaling pathway are detected in a substantial percentage of sporadic RMS (Wexler and Helman, 1997; Ragazzini *et al.*, 2004). Although both p53 and PTCH1 function as suppressors of tumorigenesis, the signaling pathways in which they are involved are considered to be independent. So far, no study has established an association between the *p53* or *PTCH1* status with the gene expression profiles and resulting histological subtypes of RMS, although this might have a profound impact on the treatment of this tumor.

Due to the low frequency of either syndrome in humans, we have performed expression profiling on tumors derived from murine models of LFS and NBCCS. Heterozygous *p53*$^{+/-}$ mutant mice develop a number of sarcomas, including RMS (Harvey *et al.*, 1993; Jacks *et al.*, 1994). RMS are also prevalent in heterozygous *Ptch1*$^{neo67/+}$ animals (Calzada-Wack *et al.*, 2002). We show that the RMS encountered in these mice differ in their gene expression patterns and investigate the link between these profiles and their genetic etiology.

Results

Ptch1- *and* p53-*dependent RMS differ extremely in the time of onset and incidence*

To exclude possible effects of the different genetic backgrounds on molecular signature of RMS that arise in *Ptch1*$^{neo67/+}$ and *p53*$^{+/-}$ mice, we first bred the targeted mutations onto a common genetic background by crossing CD-1 *Ptch1*$^{neo67/+}$ (Hahn *et al.*, 1998) with C57BL/6 *p53*$^{+/-}$ mice (Jacks *et al.*, 1994). The resulting offspring was examined weekly for tumor formation over a period of 550 days. As shown in Figure 1,
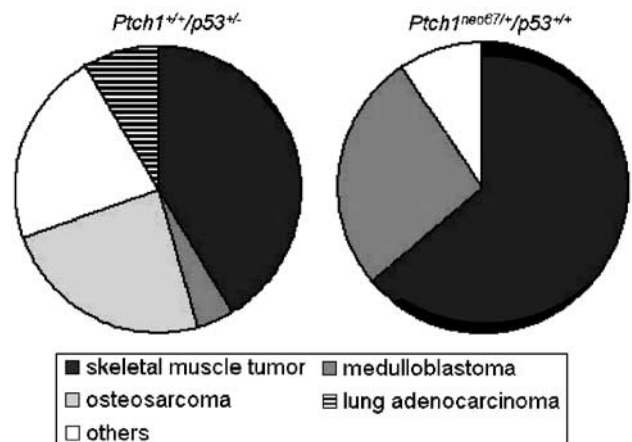
heterozygosity for *Ptch1* dramatically increases the incidence of tumors arising from skeletal muscle (SMTU = *s*keletal *m*uscle *tu*mor). Note that not all of the SMTU were histologically confirmed as RMS. Out of 96 animals with the *Ptch1*$^{neo67/+}$ genotype more than 40% developed grossly visible SMTU within 550 days of age, with a median age of onset of 224 days. Only 20% of *p53*$^{+/-}$ mice developed these tumors in this time, with a median age of onset of 329 days. Double-heterozygous *Ptch1*$^{neo67/+}$/*p53*$^{+/-}$ mutants developed SMTU with frequencies (37%) and median age of onset (228 days) comparable with the *Ptch1*$^{neo67/+}$ animals (data not shown). Irrespective of genotype, SMTU most commonly occurred in the trunk and extremities (data not shown). No SMTU were detected in wild-type littermates (data not shown). These results indicate that SMTU originating from heterozygous *Ptch1*$^{neo67/+}$ and *p53*$^{+/-}$ mice differ dramatically in the time of onset and incidence.

Other tumor types including medulloblastoma (MB), osteosarcoma (OS) and lung adenocarcinoma (LA) were observed in both genotypes. The relative frequency of tumor types in the cohorts is depicted in Figure 2. The most common tumor types in *Ptch1*$^{neo67/+}$ mice were SMTU and MB, representing 63 and 27% of total tumors, respectively. In *p53*$^{+/-}$ mice, SMTU, OS, LA and MB were observed in 41, 24, 9 and 4% of total tumors, respectively. Additionally, single cases of lymphoma, leiomyosarcoma, hemangiosarcoma, hepatocellular carcinoma and chondrosarcoma, lipoma and trichoepithelioma were found in *p53*$^{+/-}$ and *Ptch1*$^{neo67/+}$ animals, respectively.

Ptch1-*dependent RMS show a less aggressive growth and are histologically more differentiated than* p53-*dependent RMS*

We performed a comparative immunohistochemical and histological analysis of SMTU of *Ptch1*$^{neo67/+}$ and *p53*$^{+/-}$

Figure 1 Rhabdomyosarcomagenesis in *Ptch1*- and *p53*-mutant mice. 95 *p53*$^{+/-}$ and 96 *Ptch1*$^{neo67/+}$ mice were monitored for tumors arising from skeletal muscle (SMTU) over a period of 550 days. All mice were from a (CD-1 × C57BL/6) F1 hybrid background. The cumulative incidence of SMTU, corrected for confounding causes of death, is plotted as a function of age in days. Mice diagnosed with SMTU are represented by open (*p53*-mutant) and closed squares (*Ptch1*-mutant), whereas mice that died for other reasons are shown as small vertical bars

Figure 2 Tumor distribution in *Ptch1*- and *p53*-mutant mice. Pie charts show the relative frequency of tumor types observed in *p53*$^{+/-}$ and *Ptch1*$^{neo67/+}$ mice. Frequencies were determined from 46 and 63 total tumors in *p53*$^{+/-}$ and *Ptch1*$^{neo67/+}$ mice, respectively. Animals were monitored for tumors over a period of 550 days

Table 1 Immunohistochemical and histological analysis of *Ptch1*- and *p53*-dependent RMS

No.	Genotype	CD31	SMA	Desmin	Bcl-2	Ki-67	Differentiation
3	$Ptch1^{neo67/+}$	−	−	+ +	+ +	+	1
6	$Ptch1^{neo67/+}$	−	−	+ +	+ + +	+	1
13	$Ptch1^{neo67/+}$	−	−	+ +	+ +	+	2
15	$Ptch1^{neo67/+}$	−	−	+ +	+ +	+ +	1
16	$Ptch1^{neo67/+}$	−	−	+ +	+ +	+	1
461	$p53^{+/−}$	−	−	+ + +	+ + +	+ + +	2
562	$p53^{+/−}$	−	−	+ + +	+ + +	+ + +	3
728	$p53^{+/−}$	−	−	+ + +	+ +	+	1
908	$p53^{+/−}$	−	−	+ + +	+ + +	+ + +	3
957	$p53^{+/−}$	−	−	+ + +	+ + +	+ +	2

+ + + = >30% of cells positive; + + = between 10–30% of cells positive; + = <10% of cells positive; − = negative; 1 = highly differentiated; 2 = moderately differentiated; 3 = undifferentiated

mice (Table 1). Since it is known that heterozygous $p53^{+/−}$ mutant mice develop a variety of sarcomas including RMS, hemangiosarcoma and leiomyosarcoma (Harvey *et al.*, 1993; Jacks *et al.*, 1994), we first excluded the latter two tumor types by staining with hematoxylin and eosin (H&E) and relevant markers, namely CD31 and smooth muscle actin (SMA) (Coindre, 2003). As shown in Table 1, all tumors examined were negative for these two markers. Next, we stained for desmin, a widely used marker for RMS (Coindre, 2003), and found strong expression in all tumors examined, with desmin-positive cells more prevalent in *p53*-dependent RMS. In addition, we stained for the antiapoptotic protein Bcl-2, which has recently been shown to be strongly expressed in 36% of human RMS, as well as in all cases of murine *Ptch1*-associated RMS (Boman *et al.*, 1997; Kappler *et al.*, 2003). We found high levels of Bcl-2 protein in RMS from both $Ptch1^{neo67/+}$ and $p53^{+/−}$ mice. Taken together these data identify the tumors under investigation as RMS that express the RMS-specific marker desmin and in addition Bcl-2 at similar levels.

Next, we examined biological parameters of the RMS from both genotypes. Proliferative activity was evaluated using the proliferation marker Ki-67 and histological analysis performed on H&E-stained tumor sections. A low density of Ki-67-positive proliferating tumor cells was seen in four out of five *Ptch1*-dependent RMS (Figure 3c, Table 1). This was associated with a higher degree of histological differentiation, as indicated by tumor cells with a broad cytoplasm and focal striation (Figure 3a), and with positive staining for desmin (Table 1). In contrast, *p53*-dependent RMS generally displayed a much more aggressive growth, with a high density of Ki-67 positive tumor cells, being present in four out of five RMS (Figure 3d), which correlated with poor histological differentiation characterized by small spindle-shaped desmin-positive tumor cells (Table 1), absence of further cytoplasmic differentiation and a high percentage of mitotic figures (Figure 3b). One RMS of $p53^{+/−}$ origin (No. 728) displayed well-differentiated tumor cells with a very low number of Ki-67-positive tumor cells, thus resembling the *Ptch1*-associated tumor phenotype (Table 1). These results demonstrate that in general the *Ptch1*-dependent
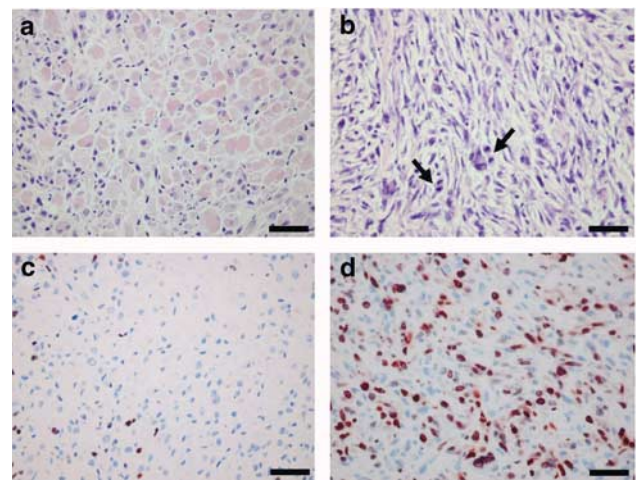
Figure 3 Differentiation and proliferation properties in *Ptch1*- and *p53*-dependend RMS. (**a** and **b**) Representative photomicrographs of H&E-stained *Ptch1*-dependent (**a**) and *p53*-dependent RMS (**b**). Arrows show mitotic figures. (**c** and **d**) Representative immunohistochemical stainings for Ki-67 of formalin-fixed, paraffin-embedded tissue sections of murine RMS of $Ptch1^{neo67/+}$ (**c**) and $p53^{+/−}$ origin (**d**). Scale bars: (**a–d**), 50 μm

RMS show a less aggressive growth and are histologically more differentiated than *p53*-dependent RMS.

p53 signaling is preserved in RMS of Ptch1$^{neo67/+}$ *mutants*

Mutations in the *p53* gene have been detected in nearly 50% of all cases of human RMS (Mulligan *et al.*, 1990; Stratton *et al.*, 1990; Felix *et al.*, 1992). In addition, it has been proposed that loss of *p53* also plays a crucial role in the genesis of MB in $Ptch1^{+/−}$ mice (Wetmore *et al.*, 2001). We therefore investigated whether p53 signaling was disturbed in RMS of $Ptch1^{neo67/+}$ mice. The analysis of *p53* cDNA revealed no mutations in the coding region of *p53* in any of the five tumors examined (data not shown). As it is generally assumed that mutations in the *p53* gene are frequently associated with an increase in stability of the p53 protein in human tumors (May and May, 1999), we investigated p53 protein levels by means of immunohistochemistry of

formalin-fixed, paraffin-embedded tissue sections of five RMS of heterozygous $Ptch1^{neo67/+}$ mice. Immunostaining using a monoclonal antibody against p53 revealed no accumulation of p53 protein in any of the tumor cases examined (data not shown).

To assess the status of the p53 signaling pathway in RMS of *Ptch1* mutants, we investigated the expression of two downstream targets of p53 ($p21^{cip1/waf1}$ and *Bax*) and of *p53* itself. Using quantitative RT–PCR we observed elevated levels of *p53* transcripts in all RMS analysed (Figure 4a). Furthermore, we detected highly
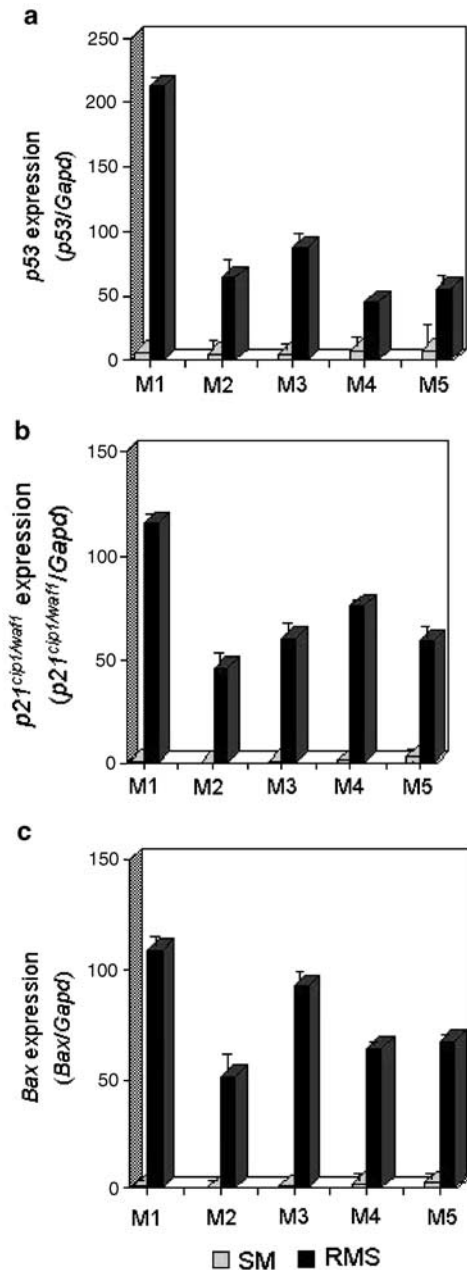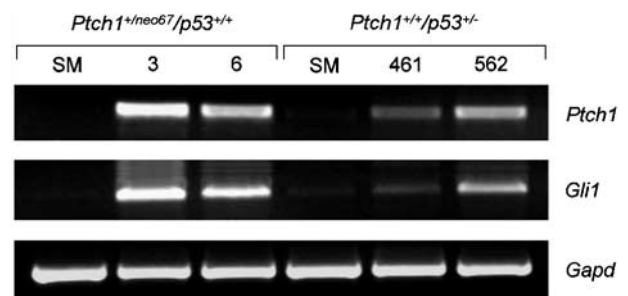
elevated transcript levels of $p21^{cip1/waf1}$ (Figure 4b) and *Bax* (Figure 4c). These results indicate that p53 signaling is activated in tumors of $Ptch1^{neo67/+}$ mice, and suggested a wild-type function of p53 in tumor tissue. Moreover, our findings clearly demonstrate that RMS formation in heterozygous $Ptch1^{neo67/+}$ mice is not dependent on mutation of *p53*.

Moderate activation of Hedgehog/Patched signaling in RMS of $p53^{+/-}$ mutants

Mutation of *Ptch1* results in the inappropriate activation of the Hedgehog/Patched signaling pathway characterized by overexpression of *Gli1* and loss of *Ptch1* itself (Ruiz i Altaba *et al.*, 2002). In order to determine whether the Hedgehog/Patched signaling pathway was also affected in RMS of $p53^{+/-}$ mutants, we performed semiquantitative RT–PCR of *Gli1* and *Ptch1*. As shown in Figure 5, the expression of both genes was elevated in the tumor tissues compared to the corresponding normal skeletal muscle (SM). As expected, the expression levels of both genes were significantly higher in the RMS tumors derived from $Ptch1^{neo67/+}$ mice (Figure 5).

Rhabdomyosarcomagenesis in heterozygous $p53^{+/-}$ mice does not involve loss of the wild-type *p53* allele

Both retention (Venkatachalam *et al.*, 1998) and loss of the wild-type allele (Jacks *et al.*, 1994) has previously been described in tumors arising in $p53^{+/-}$ mice. Therefore, we checked whether loss of both *p53* alleles is necessary for tumor formation in $p53^{+/-}$ mice and whether the remaining wild-type *p53* allele was deleted in RMS tissue derived from these mice. Using the reverse primer RT-p53 in conjunction with the primer p53-2 localized in exon 4 of *p53* (deleted in the targeted *p53* allele), a band of the appropriate size was detected in all tumors by semiquantitative RT–PCR (supplementary Figure A). The remaining wild-type allele was sequenced in four RMS of heterozygous $p53^{+/-}$ mice. No mutations were detected in any of the samples examined (data not shown). These results demonstrate

Figure 4 Activation of components of the p53 signaling pathway. Quantification of transcript levels of (**a**) *p53*, (**b**) $p21^{cip1/waf1}$ and (**c**) *Bax* in normal SM and RMS of five $Ptch1^{neo67/+}$ heterozygous mice (M1–M5) monitored by quantitative RT–PCR

Figure 5 Hedgehog/Patched signaling in *Ptch1-* and *p53*-dependent RMS. *Gli1* and *Ptch1* expression was analysed in SM and RMS of $p53^{+/-}$ and $Ptch1^{neo67/+}$ mice using semiquantitative RT–PCR, respectively. *Gapd* expression was monitored to control for the amount of sample RNA

that the wild-type *p53* allele was retained in tumor tissue.

Expression profiling distinguishes between Ptch1- *and* p53-*dependend RMS*

To determine if the specific gene defects lead to particular molecular changes during rhabdomyosarcomagenesis, we profiled gene expression of RMS of each genotype using SM tissue and C2C12 myoblasts as non-neoplastic controls. To this end, Cy5-labeled cDNA probes prepared from each test RNA sample and Cy3-labeled reference cDNA probes prepared from a pool of RNAs isolated from eight different mouse tissues were co-hybridized to Agilent's mouse cDNA microarrays containing 8400 mouse genes, including ∼3700 characterized genes from the Mouse UniGene database and ∼4700 nonannotated EST clones. The fluorescence ratio was quantified for each gene and reflected the relative abundance of the gene in each test RNA sample compared with the reference RNA pool. The use of a common reference probe allowed us to treat these fluorescent ratios as measurements of the relative expression level of each gene across all 13 samples. Data restriction left 2852 genes (∼34%) in the data set, which is available as a supplementary Table A. A hierarchical clustering algorithm was used to group tumor samples on the basis of similarities in their expression of these genes. As depicted in Figure 6, RMS and SM of heterozygous *Ptch1*$^{neo67/+}$ mice and the C2C12 cells clustered into one group, whereas RMS of heterozygous *p53*$^{+/-}$ mice were clustered as a second group. Furthermore, the same algorithm was used to cluster genes on the basis of similarity in the pattern with which their expression varied over all samples. The data are shown in a matrix format (Figure 6), with each row representing all the hybridization results for a single cDNA element of the array, and each column representing the measured expression levels of all genes in an individual sample. One of the clearest distinctions in the gene expression patterns of the two RMS subtypes are the subset of genes that are known as myogenic markers (Figure 6, middle panel) including *myosin heavy polypeptide 1*, *tropomyosin 2 beta*, *troponin I* and *troponin T3*. This group of genes was more highly expressed in *Ptch1*-associated RMS than in *p53*-associated RMS. The same set of genes was strongly expressed in SM tissue, but not in C2C12 cells. Another interesting cluster of genes sharing differentially expression between the two RMS subtypes contained genes associated with Hedgehog/Patched signaling (Figure 6, upper panel), namely *Igf2* (Hahn *et al.*, 2000), forkhead box gene *Foxf1* (Kappler *et al.*, 2003), the growth arrest and DNA-damage-inducible gene *Gadd45a* (Kappler *et al.*, 2004), and *caveolin 3* (*Cav3*) (Karpen *et al.*, 2001). These genes generally exhibited higher transcript levels in *Ptch1*-dependend RMS rather than in *p53*-dependend RMS or SM tissue and C2C12 cells. A cluster displaying genes with higher transcript levels in *p53*-dependend RMS contained the cell cycle-associated genes *cyclin B1* (*Ccnb1*), *activator of S phase kinase* and the proliferation

marker *Ki-67* (Figure 6, lower panel). These genes were also strongly expressed in C2C12 cells, but displayed only low levels in SM tissue.

By compiling sets of genes that vary significantly in their mean relative expression between the two RMS subtypes (Tables 2 and 3), we detected several genes previously associated with rhabdomyosarcomagenesis or myogenic differentiation, namely *Fos* (Fleischmann *et al.*, 2003), *myogenic differentiation 1 (MyoD1)* (Kablar *et al.*, 2003), *Junb* (Chalaux *et al.*, 1998), *follistatin* (Amthor *et al.*, 2002; Armand *et al.*, 2003), *heparin binding epidermal growth factor-like growth factor* (Chen *et al.*, 1995), *matrix metalloproteinase 9* (Kherif *et al.*, 1999) and *p21*$^{cip1/waf1}$ (see Figure 4b). These genes generally displayed higher transcript levels in *Ptch1*-dependend RMS than in *p53*-dependend RMS (Table 2). On the other hand, we detected several genes like *catenin beta*, *cadherin 2*, *cyclin-dependent kinase 4* (*Cdk4a*), *biglycan* and *platelet-derived growth factor C* that were expressed at significant higher levels in *p53*-dependend RMS than in *Ptch1*-dependend RMS (Table 3).

A number of the candidate genes identified by microarray analysis were validated by semiquantitative RT–PCR. As shown in Figure 7, the expression of *MyoD1*, *Igf2*, *Foxf1*, *Cav3* and *Gadd45a* was increased, whereas the expression of *Cdk4* and *Ccnb1* was decreased in *Ptch1*-dependend RMS compared to *p53*-dependend RMS. Altogether, microarray analysis revealed distinct gene expression signatures in *Ptch1*- and *p53*-derived RMS.

Discussion

The goal of this study was to gain insight into the molecular events that drive *p53*- or *Ptch1*-dependent rhabdomyosarcomagenesis, and to establish their characteristic molecular signatures. To this end, we compared biological, histological and molecular profiles of RMS arising in mice bearing targeted genetic defects in *p53* and *Ptch1*. To confirm the respective genetic defects, we firstly have verified the allelic status of each tumor suppressor gene in the respective tumors. We also ruled out severe alterations of p53 signaling in *Ptch1*-associated and of Hedgehog/Patched signaling in *p53*-associated tumors. However, some feature are shared by both tumor subtypes, notably expression of markers for RMS such as desmin and Bcl-2 (Boman *et al.*, 1997; Merlino and Helman, 1999; Kappler *et al.*, 2003), and the pattern of distribution of tumors to the trunk and extremities. The subtypes differed from each other in several points. RMS of *Ptch1* heterozygous mice were histologically well differentiated with a low proliferation index, whereas *p53*-dependent RMS generally display a more aggressive and less differentiated small blue round cell phenotype. Moreover, the two RMS subtypes differ in the time of onset and incidence.

Most importantly, the two murine RMS subtypes differed dramatically in their gene expression profiles. The specific transcriptional signature of each tumor can
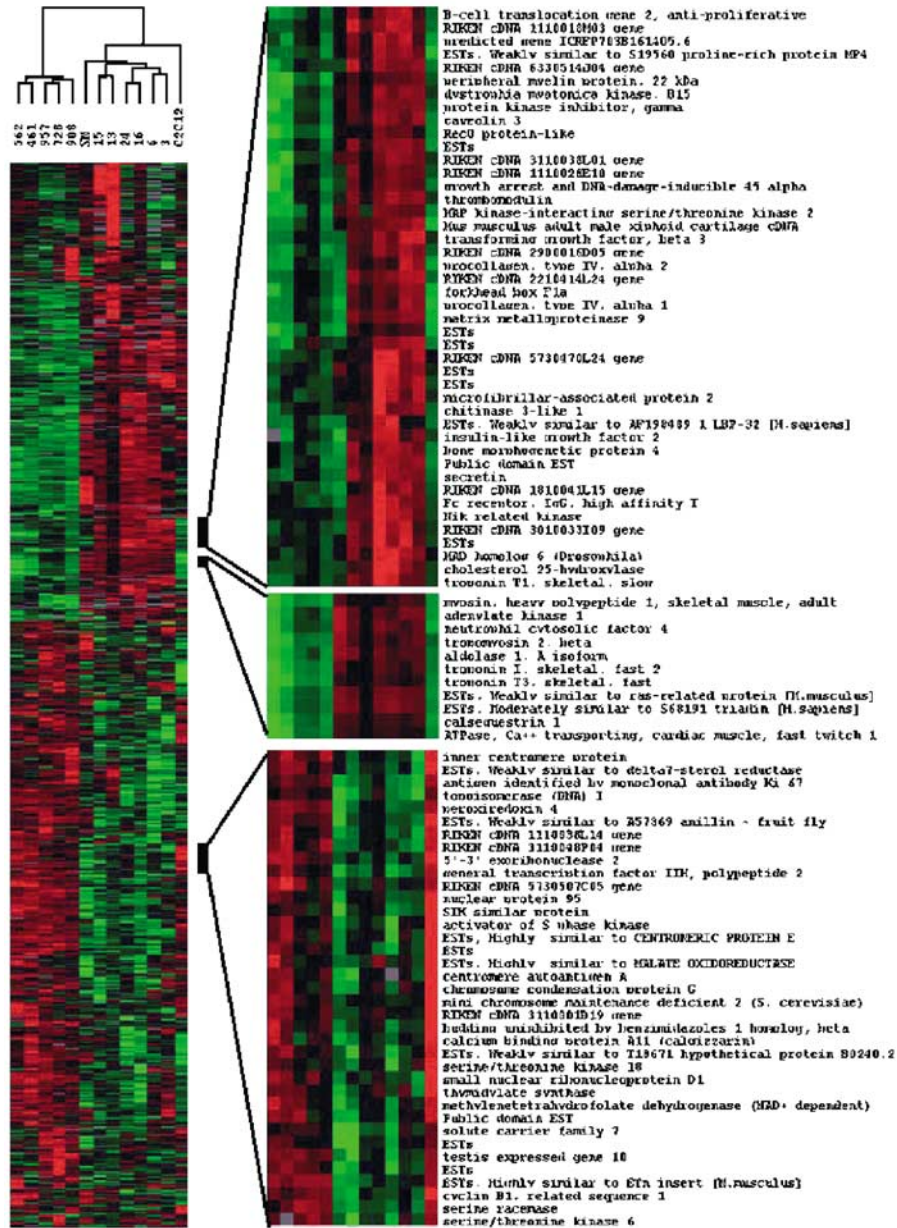
Figure 6 Two-way hierarchical clustering of gene expression data. Each row represents a separate cDNA clone on the microarray and each column a separate tumor sample. The colorgram depicts high (red) and low (green) relative levels of gene expression for each tumor sample compared to a universal reference RNA sample, with color saturation signifying the degree of gene expression. Gray indicates missing or excluded data. The top dendrogram lists the samples studied, and provides a measure of the relatedness of gene expression in each individual sample. There were two principle branches, one containing RMS and SM of heterozygous *Ptch1*^neo67/+^ mice (Nos. 3, 6, 13, 15, 16 and 24) as well as C2C12 cells, and the other containing RMS of heterozygous *p53*^+/−^ mice (Nos. 461, 562, 728, 908 and 956). An enlarged view of three gene clusters is shown to the right of the diagram. The upper cluster comprises genes associated with Hedgehog/Patched signaling and the middle cluster myogenic markers, both with a high relative gene expression in *Ptch1*-associated RMS. The lower cluster contains cell cycle-associated genes with a high relative gene expression in *p53*-associated RMS

be summarized as follows: (i) RMS of heterozygous *Ptch1*^neo67/+^ mice show higher transcript levels of known myogenic differentiation markers; (ii) *p53*-dependent RMS exhibit stronger expression of cell cycle-associated genes; and (iii) transcripts of genes described to play a role in Hedgehog/Patched signaling are more abundant in RMS of heterozygous *Ptch1*^neo67/+^ mice. These findings are consistent with previous observations in human and murine RMS.

First, using cDNA microarray analysis on human RMS cell lines with different differentiation properties, it has been described that almost half of the genes with higher expression in more differentiated RMS cells were markers of terminal myogenic differentiation, such as

**Table 2** Selected genes highly expressed in *Ptch1*-dependent RMS

GenBank Acc. No.	Gene name	Fold difference	P-value
Muscle-related genes			
AA770924	Troponin T3, skeletal, fast	147.1	0.001
AA821941	Troponin I, skeletal, fast 2	101.6	0.001
AA656712	Myosin, heavy polypeptide 1, skeletal muscle, adult	75.2	0.001
AA821970	Myosin light chain, phosphorylatable, fast skeletal muscle	42.1	0.001
AA656407	Troponin T1, skeletal, slow	12.9	0.001
W18330	Tropomyosin 2, beta	12.6	0.001
AA437694	Myogenic differentiation 1	11.0	0.001
AA822257	Myosin light chain, alkali, fast skeletal muscle	2.9	0.005
AA770902	Actin, alpha 1, skeletal muscle	2.8	0.006
Hedgehog/Patched signaling-associated genes			
AA002425	Caveolin 3	12.7	0.001
AI326605	Cyclin-dependent kinase inhibitor 1A (p21)	9.0	0.001
AI322387	Insulin-like growth factor 2	7.5	0.006
AA553242	Growth arrest and DNA-damage-inducible 45 alpha	3.0	0.015
AA117969	Forkhead box F1a	2.5	0.015
Miscellaneous genes			
W14436	Matrix metalloproteinase 9	8.8	0.001
AA726638	Follistatin	8.2	0.001
AA545284	MAD homolog 7 (Drosophila)	7.4	0.001
AI427265	MAD homolog 6 (Drosophila)	7.3	0.001
AA608298	Jun-B oncogene	6.3	0.001
AI893912	Sine oculis-related homeobox 1 homolog (Drosophila)	5.7	0.001
AI595201	Heparin binding epidermal growth factor-like growth factor	4.2	0.001
AA002910	FBJ osteosarcoma oncogene	3.9	0.004

Table 3 Selected genes highly expressed *p53*-dependent RMS

GenBank Acc. No.	Gene name	Fold difference	P-value
Growth-associated genes			
AI892404	Cyclin-dependent kinase 4	19.6	0.001
AA028539	Platelet-derived growth factor, C polypeptide	6.1	0.007
AA450523	Cyclin B1, related sequence 1	5.2	0.001
AA671317	Antigen identified by monoclonal antibody Ki 67	4.0	0.001
AA067144	Activator of S phase kinase	3.5	0.005
W78296	Mitogen-activated protein kinase 14	3.3	0.016
AI893985	Mitogen-activated protein kinase 10	2.8	0.017
AA238356	Hepatocyte growth factor-like	2.7	0.016
Miscellaneous genes			
AA855996	Biglycan	6.3	0.003
AA980366	Vitronectin	5.4	0.001
W64107	Bcl-associated death promoter	5.0	0.004
W14224	N-myc downstream regulated 1	4.8	0.001
AA242226	Cadherin 2	4.2	0.017
AA178068	Zinc-finger homeobox 1a	3.5	0.012
AA066458	Cadherin 16	3.4	0.003
W70696	Avian reticuloendotheliosis viral oncogene homolog A	3.1	0.002
AI386280	Caspase 8	3.0	0.011
AA982280	N-myc (and STAT) interactor	2.8	0.002
AA822077	Catenin beta	2.7	0.001

isoforms of myosin, actin and troponin. Genes more abundantly expressed by undifferentiated RMS cells are markers of the mesenchymal lineage or of early myogenic commitment (Astolfi *et al.*, 2001). Thus, it can be inferred that RMS of heterozygous *Ptch1*[neo67/+] mice arise from skeletal muscle precursor cells that are blocked very late in their terminal muscle differentiation, resulting in the high expression of late markers of differentiation. This conclusion is furthermore strengthened by our findings that *Ptch1*-dependent RMS and normally differentiated SM tissue display similar levels of muscle-specific gene expression, in contrast to the situation found in proliferating C2C12 myoblasts, which represent multipotent mesenchymal
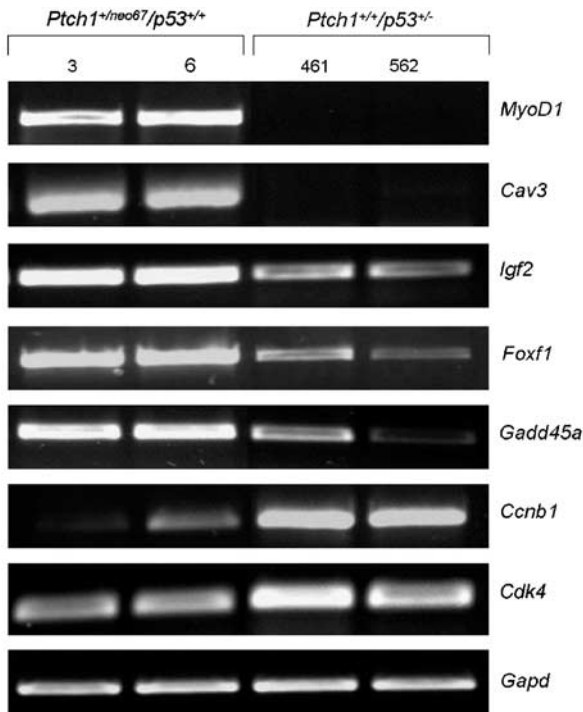
Figure 7 Verification of microarray findings. To confirm the expression profile for genes obtained from the cDNA microarray analysis, the expression level of selected genes from Tables 2 and 3 was examined in RMS of *Ptch1^neo67/+* and *p53^+/−* heterozygous mice by means of semiquantitative RT–PCR. *Gapd* expression was monitored to control for the amount of sample RNA

precursor cells retaining the ability to differentiate into osteoblasts, adipocytes or myotubes under appropriate culture conditions (Wada *et al.*, 2002).

Second, using again cDNA microarray analysis it has been demonstrated that differentiating C2C12 myoblasts, a well-established *in vitro* model for muscle differentiation, show expression patterns consistent with cell cycle withdrawal (Shen *et al.*, 2003). Compared with proliferating cells, differentiating myotubes exhibited a strong decrease in cell cycle-associated genes such as *Ccnb1* and *Cdk4*. Since we found high expression levels of these genes in *p53*-dependent RMS, it is highly probable that this more aggressive subtype arises through the maintenance of proliferative activity of mesenchymal myogenic progenitor cells, and through a block of these cells very early in terminal muscle differentiation, as evidenced by the low expression of appropriate markers. This assumption is strengthened by our finding that both SM, which is a G0 phase tissue, as well as the well-differentiated *Ptch1*-dependent subtype of RMS, lack expression of relevant cell cycle-associated genes.

Third, the relative abundance of genes such as *Igf2*, *Foxf1*, *Gadd45a* and *Cav3* in RMS of heterozygous *Ptch1^neo67/+* mice in comparison to tumors of *p53^+/−* mice is consistent with their involvement in Hedgehog/Patched signaling (Hahn *et al.*, 2000; Karpen *et al.*, 2001; Kappler *et al.*, 2003, 2004). It has previously been described that *Igf2* is highly expressed in RMS of

heterozygous *Ptch1^neo67/+* mice, and that it is indispensable for tumor formation (Hahn *et al.*, 2000). Furthermore, LOH or LOI at the 11q15 locus, a region harboring the human *IGF2* gene, is characteristic for human ERMS, and may contribute to the overexpression of *IGF2* observed in these tumors (Zhan *et al.*, 1994). Thus, *IGF2* expression may provide a good marker for a less aggressive and prognostically favorable subtype of RMS. Caveolins interact with signaling molecules in a number of key pathways, including endothelial nitric oxide synthase, src family tyrosine kinases, ras, protein kinase A (Couet *et al.*, 2001) and Ptch1 (Karpen *et al.*, 2001). Whereas *Cav1* has already been widely implicated as a tumor suppressor gene, data on *Cav3* and its role in carcinogenesis are limited. Significantly, *Cav3* expression is confined to muscle cells, and it has been suggested that Cav3 has a specialized role associated with the differentiated state in this cell type (Doyle *et al.*, 2003). Thus, the higher expression of *Cav3* in RMS of heterozygous *Ptch1^neo67/+* mice is consistent with the higher differentiation properties of this tumor subtype, rather than an indication for regulation of this gene by an activated Hedgehog/Patched pathway.

Another gene that was upregulated in *Ptch1*-associated RMS is *p21^cip1/waf1*. In humans, *p21^cip1/waf1* expression has been demonstrated to be higher in ERMS compared with ARMS (Moretti *et al.*, 2002). It is known that expression of this cell cycle inhibitor is under the control of multiple transcriptional factors, including p53 and MyoD1. In our study the function of the p53 signaling pathway may even be preserved and seems to be activated in *Ptch1*-associated RMS, probably as a result of the cellular regulatory network to protect the organism by stimulating growth arrest and apoptosis. However, as *MyoD1* expression was also increased in these tumors (see Table 2) we cannot ascertain whether the elevated levels of *p21^cip1/waf1* are the result of p53 or MyoD1 expression.

An assignment of the *Ptch1-* and *p53*-dependent subtypes to one specific human form of RMS is clearly not possible at that stage, since the gene expression profiles of the latter have yet to be investigated. However, the differentiation properties, histology, expression of terminal myogenic differentiation markers, and expression of *Igf2* and *p21^cip1/waf1* in RMS of *Ptch1^neo67/+* mice mostly associated with human ERMS. The earlier occurrence of *Ptch1*-dependent RMS is consistent with such a suggestion (Wexler and Helman, 1997). The less differentiated phenotype with small round densely packed cells and the high expression levels of cell cycle-associated genes of the p53-dependent RMS resembles human ARMS, which occur in an older age group (Merlino and Helman, 1999). If the gene profile is found and confirmed in human RMS, these differences may have significance for the treatment of this cancer. Given that (a) p53 is required for the induction of apoptotic cell death by ionizing radiation and some types of chemotherapeutic drugs (May and May, 1999); (b) Hedgehog/Patched signaling can be specifically blocked by either the alkaloid cyclopamine

(Taipale *et al.*, 2000) or inhibitory small molecules (Williams *et al.*, 2003); (c) Igf2 accumulation can be selectively targeted by a methylated oligonucleotide inhibition strategy (Yao *et al.*, 2003); and (d) butyrate can be used to induce an increase of cell cycle inhibitors like $p21^{cip1/waf1}$ and thereby induce growth inhibition in RMS cells (Moretti *et al.*, 2002), classification of RMS on the basis of expression information may serve as a step toward defining a new molecular taxonomy of this solid childhood cancer, resulting in the development of gene mutation- and expression-specific therapies. The study presented here is a first step towards such a classification.

Materials and methods

Mouse breedings and crosses

Animal experiments were performed according to all necessary legal requirements. Mice heterozygous for $Ptch1^{neo67/+}$ and $p53^{+/-}$ on a mixed C57BL/6 × CD-1 background were genotyped according to published PCR protocols (Jacks *et al.*, 1994; Hahn *et al.*, 1998), except that the primer W3′ used for amplification of both the wild-type and the mutant p53 allele was 5′-TGGTATACTCAGAGCCGGCCT-3′. Mice were monitored for tumor formation weekly.

Tissue specimens

Tumors were surgically removed from muscle tissue and cut into two parts. Specimens to be used for isolation of total RNA (see below) were immediately frozen in liquid nitrogen. The remainder was formalin-fixed and embedded in paraffin for immunohistochemical analysis. The identity of the tumors was established on H&E stained sections by a trained pathologist. Only RMS tissues containing > 95% tumor cells were used in this study.

Immunohistochemistry

For immunohistochemical analyses 3-μm-thick paraffin sections were mounted on organo-silane coated slides. After deparaffination and rehydration the endogenous peroxidase activity was quenched with 3% hydrogen peroxide. For antigen retrieval the tissue sections were either microwaved in citrate buffer at 700 W for 15 min (for antibodies 1 and 4) or digested with protease XXIV for 20 min at 37°C (for antibodies 2, 3 and 5). Primary antibodies were diluted in Tris-buffered saline (pH 7.5) containing 5% bovine serum albumin. The antibody panel included: (1) monoclonal mouse anti-Ki-67 (Novacastra Laboratories, Newcastle upon Tyne, UK) diluted 1 : 50; (2) monoclonal mouse anti-Desmin (Sigma, Munich, Germany) diluted 1 : 50; (3) monoclonal mouse anti-human CD31 (Dianova, Hamburg, Germany) diluted 1 : 50; (4) polyclonal rabbit anti-human Bcl-2 (Santa Cruz Biotechnology, Santa Cruz, CA, USA) diluted 1 : 40; and (5) monoclonal mouse anti-p53 (Santa Cruz Biotechnology) diluted 1 : 100. After incubation of the sections with the primary antibodies and subsequent incubation for 30 min with Envision™-Peroxidase (DakoCytomation, Hamburg, Germany), signals were detected with diaminobenzidine and counterstained with hematoxylin. Smooth muscle actin was labeled using a monoclonal mouse anti-SMA antibody directly conjugated with alkaline phosphate (Sigma) diluted 1 : 50 and nitro tetrazolium blue/5-bromo-4-chloro-indolyl phosphate as chromogen.

Isolation of RNA

Total RNA was extracted from RMS and normal SM tissue of heterozygous $Ptch1^{neo67/+}/p53^{+/+}$ and $Ptch1^{+/+}/p53^{+/-}$ mice of the F1 generation, C2C12 myoblasts (American Type Culture Collection, Manassas, VA, USA) grown for 72 h in growth medium (DMEM supplemented with 10% FCS), and from various other tissues (kidney, liver, spleen, muscle, brain, lung, testis, heart) of wild-type mice using TRIZOL reagent (Invitrogen, Carlsbad, CA, USA). Total RNA of the latter tissues was pooled and used as a universal reference RNA in cDNA microarray experiments. For these experiments total RNA was further purified using RNeasy columns (Qiagen, Hilden, Germany). The quality of RNA was checked by the 2100 bioanalyser (Agilent Technologies, Palo Alto, CA, USA) using the RNA 6000 Nano LabChip Kit (Agilent Technologies).

cDNA microarray analysis

The gene expression profiles of RMS of heterozygous $Ptch1^{neo67/+}$ and $p53^{+/-}$ mice, SM of a heterozygous $Ptch1^{neo67/+}$ mouse as well as C2C12 cells were determined using mouse cDNA microarray kits purchased from Agilent Technologies. Briefly, equal amounts (20 μg) of total RNA from universal reference and test samples were each reverse-transcribed in a total volume of 50 μl with 2 μg oligo(dT)$_{12-18}$ primers and 400 U SuperScriptII reverse transcriptase (Invitrogen) in the presence of 0.025 mM Cy3- or Cy5-dUTP (NEN Life Science Products, Boston, MA, USA). After 2 h incubation at 42°C, the reaction was stopped by heating for 10 min at 70°C. Template RNA was degraded by incubating with RNase H (Roche Diagnostics, Mannheim, Germany) for 30 min at room temperature. Unincorporated nucleotides were removed from labeled cDNA using QIAquick PCR purification columns (Qiagen). The differentially labeled cDNAs from the reference and test samples were combined, 2.5 μg mouse C_0t1 DNA (Invitrogen) was added, and the mix was dried to completion. The probe was resuspended in 25 μl deposition hybridization buffer (Agilent Technologies), denatured for 5 min at 95°C and hybridized overnight at 65°C to mouse cDNA microarrays under a lifterslip (Erie Scientific Company, Portsmouth, NH, USA) in a hybridization chamber (Scienion, Berlin, Germany). After hybridization, slides were washed 3 × 5 min in 0.5 × SSC/0.01% SDS and 1 × 5 min in 0.06 × SSC with moderate agitation. Slides were quickly transferred into swinging buckets in a benchtop centrifuge and dried for 2 min at 400 g. The fluorescent signal of hybridized molecules was detected for Cy3 (universal reference) and Cy5 (test sample) using Agilent's dual-laser Microarray Scanner and data acquisition was performed with the G2566AA Feature Extraction software (Agilent Technologies). This software was furthermore used to subtract the local background from the features and to normalize the data by utilizing a method that is based on rank-ordered consistency. The resulting data were used to calculate the ratio of gene expression in test sample *versus* the universal reference. These relative gene expression values were used to calculate the average relative gene expression of six *Ptch1* and five *p53* tumors, respectively. Fold changes were determined (average of *Ptch1*-mutant tumor samples/average of *p53*-mutant tumor samples) and the data set was restricted by using at least a two-fold difference as a filter cutoff. The selected group of genes was examined by hierarchical cluster analysis to find subgroups of genes based

on similar expression patterns. Preceding the clustering analysis all ratio values were log-transformed (base 2) and filtered to reach 70% presence of cases. We applied hierarchical clustering to both axes, using the weighted pair-group algorithm with a centroid average as implemented in the program CLUSTER (http://microarrays.org/software.html). The results were visualized by using the TREEVIEW matrix (http://microarrays.org/software.html). We selected candidate genes by requiring their relative gene expression levels to yield $P < 0.05$ for the standard Student's *t*-test in *Ptch1*- and *p53*-mutant RMS, as well as giving at least a two-fold increase/decrease in the gene expression ratio.

Reverse transcription–PCR

Reverse transcription of total RNA from RMS of heterozygous *Ptch1*$^{neo67/+}$ and *p53*$^{+/-}$ mice was performed using random hexamers and SuperScriptII reverse transcriptase (Invitrogen).

Semiquantitative PCR amplifications of the murine genes *MyoD1, Igf2, Foxf1, Cav3, Gadd45a, Ccnb1, Cdk4, Gli1, Ptch1* and glyceraldehyde-3-phosphate dehydrogenase (*Gapd*) were carried out with 50 ng of cDNA using the forward (F) and reverse (R) primers as follows: MyoD1-F 5′-AAAGTGAAT GAGGCCTTCGAGAC-3′ and MyoD1-R 5′-AAGCACCT GATAAATCGCATTGGG-3′; Igf2-F 5′-GACGACTTCCC CAGATACCCCGTG-3′ and Igf2-R 5′-TCACTCGATGGTT GCTGGACATCTC-3′; Foxf1-F 5′-CTCATCGTCATGGC TATCCAGA-3′ and Foxf1-R 5′-GAGGCTGTTGCTTGAT GTAGGA-3′; Cav3-F 5′-ATGATGACCGAAGAGCACAC GGAT-3′ and Cav3-R 5′-TTAGCCTTCCCTTCGCAGCAC CAC-3′; Gadd45a-F 5′-TGCAGAGCAGAAGACCGAAAG GAT-3′ and Gadd45a-R 5′-TTAAGGCAGGATCCTTCCA TTGTGA-3′; Ccnb1-F 5′-TGACAGTTACTGCTGCTTCCA AG-3′ and Ccnb1-R 5′-CTGTATTAGCCAGTCAATGAG GAT-3′; Cdk4-F 5′-GGAAACTCTGAAGCCGACCAGTT G-3′ and Cdk4-R 5′-ACTCTGCGTCGCTTTCCTCCTTG-3′; Gli1-F 5′-GGCTTTCATCAACTCTCGCTGTAC-3′ and Gli1-R 5′-AGCTTGCACACGTATGGCTTCTC-3′; Ptch1-F 5′-TTC TGCTGCCTGTCCTCTTATC-3′ and Ptch1-R 5′-GCCAGAA TGCCCTTCAGTAGAA-3′; Gapd-F 5′-ATCTTCTTGTGCA GTGCCAG-3′ and Gapd-R 5′-ATGGCATGGACTGTGGTC AT-3′. PCR reactions were performed in a 20 μl final reaction mixture for 25–28 cycles consisting of 30 s denaturation at 95°C, hybridization of primers for 30 s at 55°C and extension for 1 min at 72°C. The individual cycle number for each gene was defined by predetermining the linear range of the PCR. Amplification of *Gapd* was used as a reference standard to control for the amount of sample RNA.

Quantitative real-time PCR was carried out using an ABI PRISM 7700 sequence detector (Applied Biosystems, Foster City, CA, USA) as previously described (Calzada-Wack *et al.*,

2002). Gene-specific primers were 5′-TCTCCTCCCCTCAAT AAGCTATTC-3′ and 5′-TGGCGCTGACCCACAACT-3′ for amplification of murine *p53*, 5′-GGAACATCTCAGGG CCGAA-3′ and 5′-GCAGAAGACCAATCTGCGCTT-3′ for amplification of murine *p21*$^{cip1/waf1}$, and 5′-GTGCTCAAG GCCCTGTGC-3′ and 5′-CAGACAAGCAGCCGCTCAC-3′ for amplification of murine *Bax1*. The fluorogenic probes were 5′-CCAGCTGGTGAAGACGTGCCCTG-3′, 5′-ACGGAGG CAGACCAGCCTGACAGATT-3′ and 5′-AGTCCAGTGT CCAGCCCATGATGGTT-3′ for *p53*, *p21*$^{cip1/waf1}$, and *Bax1*, respectively. Amplification of *Gapd* as an endogenous control was performed to standardize the amount of sample RNA. The *Gapd* primers were 5′-TCCATGCCATCACTGCCA-3′ and 5′-GATGCAGGGATGATGTTCTGG-3′, and the fluorogenic probe was 5′-CAGAAGACTGTGGATGGCCCCT C-3′. PCR amplifications were carried out with the TaqMan Universal PCR Master Mix (Applied Biosystems) using 50 ng of cDNA, 200 nM of probe, and 300 nM forward and reverse primers in a 30 μl final reaction mixture. After 2 min incubation at 50°C, AmpliTaq Gold was activated by incubation for 10 min at 95°C. Each of the 50 PCR cycles consisted of 15 s denaturation at 95°C and hybridization/extension of probe and primers for 1 min at 60°C. All data shown are the average of at least two independent experiments.

Sequencing of murine p53

Murine *p53* cDNA was prepared by reverse transcription of total RNA isolated from five RMS of *Ptch1*$^{neo67/+}$ mice and from four RMS of *p53*$^{+/-}$ mice using RT-p53 primers (RT-p53-F 5′-CTGGCTGTAGGTAGCGACTA-3′ and RT-p53-R 5′-AACTTGGGCCAGGAACCACT-3′) and SuperScriptII reverse transcriptase (Invitrogen). The entire coding sequence was screened for mutations by sequencing four overlapping fragments (primers were RT-p53-F; RT-p53-R; p53-2 5′-GCCAAGTCTGTTATGTGCACG-3′; p53-3 5′-ATGTG-TAATAGCTCCTGCATGGGG-3′). Sequencing was performed using an ABI PRISM 377 DNA Sequencer (Applied Biosystems) and BLAST searches were carried out with the NCBI network service (http://www.ncbi.nlm.nih.gov/blast/blast.cgi).

References

Amthor H, Christ B, Rashid-Doubell F, Kemp CF, Lang E and Patel K. (2002). *Dev. Biol.*, **243,** 115–127.

Armand AS, Della Gaspera B, Launay T, Charbonnier F, Gallien CL and Chanoine C. (2003). *Dev. Dyn.*, **227,** 256–265.

Astolfi A, De Giovanni C, Landuzzi L, Nicoletti G, Ricci C, Croci S, Scopece L, Nanni P and Lollini PL. (2001). *Gene*, **274,** 139–149.

Boman F, Brel D, Antunes L, Alhamany Z, Floquet J and Boccon-Gibod L. (1997). *Pediatr. Pathol. Lab. Med.*, **17,** 233–247.

Calzada-Wack J, Kappler R, Schnitzbauer U, Richter T, Nathrath M, Rosemann M, Wagner SN, Hein R and Hahn H. (2002). *Carcinogenesis*, **23,** 727–733.

Chalaux E, Lopez-Rovira T, Rosa JL, Bartrons R and Ventura F. (1998). *J. Biol. Chem.*, **273,** 537–543.

Chen X, Raab G, Deutsch U, Zhang J, Ezzell RM and Klagsbrun M. (1995). *J. Biol. Chem.*, **270,** 18285–18294.

Coindre JM. (2003). *Histopathology*, **43,** 1–16.

Couet J, Belanger MM, Roussel E and Drolet MC. (2001). *Adv. Drug. Deliv. Rev.*, **49,** 223–235.

Dagher R and Helman L. (1999). *Oncologist*, **4,** 34–44.

Davis RJ, D'Cruz CM, Lovell MA, Biegel JA and Barr FG. (1994). *Cancer Res.*, **54,** 2869–2872.

Doyle DD, Upshaw-Earley J, Bell E and Palfrey HC. (2003). *Biochem. Biophys. Res. Commun.*, **304,** 22–25.

Felix CA, Kappel CC, Mitsudomi T, Nau MM, Tsokos M, Crouch GD, Nisen PD, Winick NJ and Helman LJ. (1992). *Cancer Res.*, **52,** 2243–2247.

Fleischmann A, Jochum W, Eferl R, Witowsky J and Wagner EF. (2003). *Cancer Cell*, **4,** 477–482.

Gorlin RJ. (1987). *Medicine (Baltimore)*, **66,** 98–113.

Hahn H, Wojnowski L, Specht K, Kappler R, Calzada-Wack J, Potter D, Zimmer A, Muller U, Samson E and Quintanilla-Martinez L. (2000). *J. Biol. Chem.*, **275,** 28341–28344.

Hahn H, Wojnowski L, Zimmer AM, Hall J, Miller G and Zimmer A. (1998). *Nat. Med.*, **4,** 619–622.

Harvey M, McArthur MJ, Montgomery Jr CA, Butel JS, Bradley A and Donehower LA. (1993). *Nat. Genet.*, **5,** 225–229.

Horn RC and Enterline HT. (1958). *Cancer*, **11,** 181–199.

Jacks T, Remington L, Williams BO, Schmitt EM, Halachmi S, Bronson RT and Weinberg RA. (1994). *Curr. Biol.*, **4,** 1–7.

Kablar B, Krastel K, Tajbakhsh S and Rudnicki MA. (2003). *Dev. Biol.*, **258,** 307–318.

Kappler R, Calzada-Wack J, Schnitzbauer U, Koleva M, Herwig A, Piontek G, Graedler F, Adamski J, Heinzmann U, Schlegel J, Hemmerlein B, Quintanilla-Martinez L and Hahn H. (2003). *J. Pathol.*, **200,** 348–356.

Kappler R, Heß I, Schlegel J and Hahn H. (2004). *Int. J. Oncol.*, **25,** 113–120.

Karpen HE, Bukowski JT, Hughes T, Gratton JP, Sessa WC and Gailani MR. (2001). *J. Biol. Chem.*, **276,** 19503–19511.

Kherif S, Lafuma C, Dehaupas M, Lachkar S, Fournier JG, Verdiere-Sahuque M, Fardeau M and Alameddine HS. (1999). *Dev. Biol.*, **205,** 158–170.

Lagutina I, Conway SJ, Sublett J and Grosveld GC. (2002). *Mol. Cell. Biol.*, **22,** 7204–7216.

Malkin D, Li FP, Strong LC, Fraumeni Jr JF, Nelson CE, Kim DH, Kassel J, Gryka MA, Bischoff FZ, Tainsky MA and Friend SH. (1990). *Science*, **250,** 1233–1238.

May P and May E. (1999). *Oncogene*, **18,** 7621–7636.

Merlino G and Helman LJ. (1999). *Oncogene*, **18,** 5340–5348.

Moretti A, Borriello A, Monno F, Criscuolo M, Rosolen A, Esposito G, Dello Iacovo R, Della Ragione F and Iolascon A. (2002). *Eur. J. Cancer*, **38,** 2290–2299.

Mulligan LM, Matlashewski GJ, Scrable HJ and Cavenee WK. (1990). *Proc. Natl. Acad. Sci. USA*, **87,** 5863–5867.

Ragazzini P, Gamberi G, Pazzaglia L, Serra M, Magagnoli G, Ponticelli F, Ferrari C, Ghinelli C, Alberghini M, Bertoni F, Picci P and Benassi MS. (2004). *Histol. Histopathol.*, **19,** 401–411.

Ruiz i Altaba A, Sanchez P and Dahmane N. (2002). *Nat. Rev. Cancer*, **2,** 361–372.

Scrable HJ, Witte DP, Lampkin BC and Cavenee WK. (1987). *Nature*, **329,** 645–647.

Shapiro DN, Sublett JE, Li B, Downing JR and Naeve CW. (1993). *Cancer Res.*, **53,** 5108–5112.

Shen X, Collier JM, Hlaing M, Zhang L, Delshad EH, Bristow J and Bernstein HS. (2003). *Dev. Dyn.*, **226,** 128–138.

Stratton MR, Moss S, Warren W, Patterson H, Clark J, Fisher C, Fletcher CD, Ball A, Thomas M, Gusterson BA and Cooper MK. (1990). *Oncogene*, **5,** 1297–1301.

Sun FL, Dean WL, Kelsey G, Allen ND and Reik W. (1997). *Nature*, **389,** 809–815.

Taipale J, Chen JK, Cooper MK, Wang B, Mann RK, Milenkovic L, Scott MP and Beachy PA. (2000). *Nature*, **406,** 1005–1009.

Venkatachalam S, Shi YP, Jones SN, Vogel H, Bradley A, Pinkel D and Donehower LA. (1998). *EMBO J.*, **17,** 4657–4667.

Wada MR, Inagawa-Ogashiwa M, Shimizu S, Yasumoto S and Hashimoto N. (2002). *Development*, **129,** 2987–2995.

Wetmore C, Eberhart DE and Curran T. (2001). *Cancer Res.*, **61,** 513–516.

Wexler LH and Helman LJ. (1997). *Rhabdomyosarcoma and the Undifferentiated Sarcomas*, 3rd edn. Raven-Lippincott: Philadelphia.

Williams JA, Guicherit OM, Zaharian BI, Xu Y, Chai L, Wichterle H, Kon C, Gatchalian C, Porter JA, Rubin LL and Wang FY. (2003). *Proc. Natl. Acad. Sci. USA*, **100,** 4616–4621.

Yao X, Hu JF, Daniels M, Shiran H, Zhou X, Yan H, Lu H, Zeng Z, Wang Q, Li T and Hoffman AR. (2003). *J. Clin. Invest.*, **111,** 265–273.

Zhan S, Shapiro DN and Helman LJ. (1994). *J. Clin. Invest.*, **94,** 445–448.

Supplementary Information accompanies the paper on Oncogene website (http://www.nature.com/onc).